Niobium and Tantalum Diphosphanato Complexes: Synthesis, Structure, and NMR Studies of $Cp_2MH[(PR)_2]$ (R = Ph, Cy, H)

Nola Etkin,[†] Michael T. Benson,[†,‡] Silke Courtenay,[†] Michael J. McGlinchey,[§] Alex D. Bain,[§] and Douglas W. Stephan*[,†]

Department of Chemistry and Biochemistry, University of Windsor, Windsor, Ontario, Canada N9B 3P4, and Department of Chemistry, McMaster University, Hamilton, Ontario, Canada N9B 3P4

Received March 6, 1997[⊗]

The reactions of Cp_2MH_3 (M = Nb, Ta) or Cp'_2NbH_3 ($Cp' = Me_3SiC_5H_4$) with excess primary phosphines yield the complexes $Cp_2NbH[(PPh)_2]$ (**1**), $Cp'_2NbH[(PPh)_2]$ (**2**), and $Cp_2TaH[(PR)_2]$ (R = Ph, **3**; R = Cy, **4**). Crystallographic studies of each of these compounds confirmed the *transoid* disposition of the phosphorus substituents with respect to the MP_2 ring. Reaction of Cp_2TaH_3 with white phosphorus afforded the parent complex $Cp_2TaH[(PH)_2]$ (**5**). While crystallographic characterization of **5** confirmed the formulation, it failed to reveal the orientation of the hydrogen atoms on P. Variable temperature NMR studies in conjunction with selective decoupling, 2D, NOE, and NOESY experiments were performed on compound **5**. These experiments were consistent with a *transoid* disposition of the hydrogens atoms on P at low temperature. The marked temperature dependence of the NMR data, while suggestive of a fluxional process, is more logically explained in terms of a dramatic and unusual temperature dependence of the ^{31}P chemical shifts. These results are discussed and their implications considered.

Introduction

Transition metal mediated formation of P−P bonds is a subject of continuing interest in our research group.[1−4] Although we have recently described a number of complexes of the form $Cp_2M[(PR)_2]$ and $Cp_2M[(PR)_3]$, we were certainly not the first to observe such di- and triphosphanato complexes. Ti, Zr, and Hf triphosphanato complexes were first reported in 1972[5] while it was not until 1989 that related diphosphanato species were described.[6] New synthetic routes to such complexes as well as crystallographic studies have also appeared in the more recent literature.[7] Despite the fact that such complexes have been known for 25 years, little is known of the reactivity of such di- and triphosphanato species. We recently reported that reaction of the anionic trihydride complex $[Cp^*_2ZrH_3]^-$ with primary phosphine generates the anionic species $[Cp^*_2ZrH[(PR)_2]]^-$ and subsequently $[Cp^*_2ZrH[(PR)_3]]^-$. Further reaction with excess phosphines results in the catalytic oligomerization of primary phosphines to $(PR)_5$.[3] We have subsequently shown that reaction of $Cp^*_2ZrH_2$ with phenylphosphine affords only the stoichiometric formation of $Cp^*_2Zr[(PPh)_3]$, implying the necessity of additional hydride ligand for catalysis.[8] Nonetheless, the synthesis and isolation of $[Cp^*_2ZrH_3]^-$ is difficult and fraught with capricious yields thus inhibiting the extension of this work to other main group oligomers. This problem has prompted the present investigation of reactivity of the trihydride complexes $Cp^{\dagger}_2MH_3$ ($Cp^{\dagger} = C_5H_5$, $C_5H_4SiMe_3$, M = Nb, Ta) with primary phosphines. Other workers have described related preliminary studies of Cp_2MH_3 with PPh_2H in which P−H and P−C activation is observed[9] while others have examined the reactions of niobium hydrides with chlorophosphines.[10] In the present study, P−H activation of primary phosphines or direct reaction with phosphorus of the group V trihydrides affords facile routes to diphosphanato complexes. The nature of these complexes is discussed, and the implications of these results for catalysis are considered.

Experimental Section

General Data. All preparations were done under an atmosphere of dry, O_2-free N_2 employing either Schlenk line techniques and an Innovative Technologies or Vacuum Atmospheres inert atmosphere glove box. Solvents were reagent grade, distilled from the appropriate drying agents under N_2, and degassed by the freeze-thaw method at least three times prior to use. All organic reagents were purified by conven-

[†] University of Windsor.
[‡] Visiting graduate student from the Department of Chemistry, University of Memphis, Memphis, TN, 38152.
[§] McMaster University.
[⊗] Abstract published in *Advance ACS Abstracts,* July 1, 1997.

(1) Ho, J.; Breen, T. L.; Ozarowski, A.; Stephan, D. W. *Inorg. Chem.* **1994**, *33*, 865.
(2) Hou, Z.; Breen, T. L.; Stephan, D. W. *Organometallics* **1993**, *12*, 3158.
(3) Fermin, M. C.; Stephan, D. W. *J. Am. Chem. Soc.* **1995**, *117*, 12645.
(4) Etkin, N.; Fermin, M. C.; Stephan, D. W. *J. Am. Chem. Soc.* **1997**, *119*, in press.
(5) Isseib, K.; Wille, G.; Krech, F. *Angew. Chem., Int. Ed. Engl.* **1972**, *11*, 527.
(6) Benac, B. L.; Jones, R. A. *Polyhedron* **1989**, *8*, 1774.
(7) (a) Hey-Hawkins, E. *Z. Naturforsch.* **1988**, *43B*, 1271. (b) Fromm, K.; Baum, G.; Hey-Hawkins, E. *Z. Anorg. Allg. Chem.* **1992**, *615*, 35.
(8) (a) Etkin, N.; Stephan, D. W. Unpublished results. (b) Related reactions of $Cp^*_2HfH_2$ with primary phosphines have been described: Vaughan, G. A.; Hillhouse, G.L.; Rheingold, A. L. *Organometallics* **1989**, *8*, 1760.
(9) Leblanc, J. C.; Moise, C. *J. Organomet. Chem.* **1989**, *364*, C3.
(10) (a) Nikonov, G. I. Lemenovskii, D. A.; Lorberth, J. *Organometallics* **1994**, *13*, 3127. (b) Nikonov, G. I.; Kuzmina, L. G.; Mountford, P.; Lemenovskii, D. A. *Organometallics* **1995**, *14*, 3588.

S0276-7333(97)00189-1 CCC: $14.00

tional methods. ^{1}H and ^{13}C{^{1}H} NMR spectra were recorded on a Bruker AC-300 operating at 300 and 75 MHz, respectively. Trace amounts of protonated solvents were used as references, and chemical shifts are reported relative to $SiMe_4$. ^{31}P NMR spectra were recorded on a Bruker AC-200 operating at 81 MHz and are referenced to 85% H_3PO_4. 500 MHz NMR data were obtained at the Bruker Applications laboratory in Milton, Ontario, and in the Department of Chemistry at McMaster University in Hamilton, Ontario. One- and two-dimensional ^{1}H and ^{31}P NMR simulations were carried out by using the program SIMPLTN.[11] Combustion analyses were performed by Galbraith Laboratories Inc. Knoxville, TN, or Schwarzkopf Laboratories, Woodside, NY. Throughout the text Cp refers to C_5H_5 and Cp′ to $C_5H_4SiMe_3$. Cp_2NbH_3,[10] Cp'_2NbH_3,[12] Cp_2TaH_3,[12] Cp_2TaMe_2Br,[13] and Cp_2TaMe_3[13] were prepared via literature methods. The light and air sensitive hydride complexes were stored in the dark at −35 °C.

Synthesis of $Cp_2NbH[(PPh)_2]$ (1). A solution of Cp_2NbH_3 (100 mg, 0.44 mmol) and phenylphosphine (97 mg, 0.88 mmol) in toluene (10 mL) was heated at 80 °C in a sealed flask for 5 min. The solution was filtered, concentrated to 2 mL, and cooled to −35 °C to give bright yellow crystals (143 mg, 73% yield). ^{1}H NMR (C_6D_6): δ 7.98 (dd, $|J_{H-H}| = 7$, 6 Hz, 2H), 7.86 (ddd, $|J_{H-H}| = 7$, 6, 1 Hz, 2H), 7.06 (p, $|J_{H-H}| = 7$ Hz, 4H), 6.99 (m, 1H), 6.91 (tt, $|J_{H-H}| = 7$, 1 Hz, 1H), 4.48 (d, $|J_{P-H}| = 2$ Hz, 5H), 4.32 (s, 5H), −1.63 (dd, $|J_{P-H}| = 51$, 3 Hz, 1H); ^{13}C{^{1}H} NMR (C_6D_6): δ 148.80 (dd, $|J_{P-C}| = 49$, 14 Hz), 148.07, (dd, $|J_{P-C}| = 55$, 12 Hz), 133.82−133.21 (m, Ph), 126.55, 125.61, 95.13 (d, $|J_{P-C}| = 5$ Hz), 94.17; ^{31}P NMR (C_6H_6) δ −107.45 (dd, $|J_{P-P}| = 352$ Hz, $|J_{P-H}| = 55$ Hz), −124.80 (d, $|J_{P-P}| = 352$ Hz). Anal. Calcd for $C_{22}H_{21}P_2Nb$: C: 60.02; H: 4.81; Found: C: 59.80; H:4.75.

Synthesis of $Cp'_2NbH[(PPh)_2]$ (2). A solution of Cp'_2NbH_3 (102 mg, 0.275 mmol) and phenylphosphine (60 mg, 0.55 mmol) in toluene (10 mL) was heated at 80 °C in a sealed flask for 5 min. The solution was filtered, concentrated to 2 mL, diluted with hexanes, and cooled to −35 °C to give a bright yellow powder (131 mg, 81% yield). Recrystallization from toluene at −35 °C gave yellow crystals suitable for crystallography. ^{1}H NMR (C_6D_6): δ 7.97 (m, 4H), 7.05 (m, 6H), 4.78 (m, 2H), 4.31 (m, 3H), 4.22 (m, 1H), 3.97 (m, 1H), 3.76 (m, 1H), 0.46 (s, 9H), 0.37 (s, 9H), −1.75 (dd, $|J_{P-H}| = 53$, 3 Hz, 1H); ^{13}C{^{1}H} NMR (C_6D_6): δ 148.72 (dd, $|J_{P-C}| = 50$, 14 Hz), 147.72, (dd, $|J_{P-C}| = 56$, 14 Hz), 133.66−133.05 (m, Ph), 126.61, 125.72, 110.46 (d, $|J_{P-C}| = 16$ Hz), 104.24, 102.92, 102.26, 101.86 (d, $|J_{P-C}| = 15$ Hz), 99.81, 99.05, 95.05, 92.60, 91.21, 1.10 (d, $|J_{P-C}| = 4$ Hz), 0.716; ^{31}P NMR (C_6D_6, 298 K) δ: −104.25 (dd, $|J_{P-P}| = 351$ Hz, $|J_{P-H}| = 49$ Hz), −134.96 (d, $|J_{P-P}| = 351$ Hz). Anal. Calcd for $C_{28}H_{37}P_2Si_2Nb$: C: 57.53; H: 6.38. Found: C: 57.02 ; H: 6.10.

Synthesis of $Cp_2TaH[(PPh)_2]$ (3). A solution of Cp_2TaH_3 (52 mg, 0.17 mmol) and phenylphosphine (25 mg, 0.34 mmol) in toluene (1 mL) was heated overnight at 130 °C in a sealed NMR tube. Small yellow crystals suitable for crystallography deposited on cooling. The remainder of the material was filtered, evaporated, and washed with hexane to give a yellow powder **3** (71 mg, 82% yield). ^{1}H NMR (C_6D_6): δ 7.97 (t, $|J_{H-H}| = 6$ Hz, 2H), 7.86 (dt, $|J_{H-H}| = 6$, 1 Hz, 2H), 7.09 (p, $|J_{H-H}| = 8$ Hz, 4H), 7.00 (tt, $|J_{H-H}| = 7$, 1 Hz, 1H), 6.9 (tt, $|J_{H-H}| = 7$, 2 Hz, 1H), 4.48 (d, $|J_{P-H}| = 2$ Hz, 5H), 4.33 (d, $|J_{P-H}| = 1$ Hz, 5H), −0.87 (d, $|J_{P-H}| = 44$ Hz, 1H); ^{13}C{^{1}H} NMR (C_6D_6): δ 149.90 (dd, $|J_{P-C}| = 48$, 13 Hz), 147.45, (dd, $|J_{P-C}| = 53$, 13 Hz), 134.27−133.76 (m, Ph), 126.44, 125.45, 94.05 (d, $|J_{P-C}| = 7$ Hz), 92.87 (d, $|J_{P-C}| = 4$ Hz); ^{31}P NMR (C_6H_6) δ −145.08 (dd, $|J_{P-P}| = 325$ Hz, $|J_{P-H}| = 39$ Hz), −162.75 (d, $|J_{P-P}| = 325$ Hz); ^{31}P NMR (C_7H_8, 193K) δ −152.34 (d, $|J_{P-P}| = 325$ Hz), −164.36 (d, $|J_{P-P}| = 325$ Hz); ^{31}P NMR (C_7H_8, 373K) δ −139.04 (d, $|J_{P-P}| = 329$ Hz), −160.22 (d, $|J_{P-P}| = 329$ Hz). Anal. Calcd for $C_{22}H_{21}P_2Ta$: C: 50.02; H: 4.01. Found: C: 50.00; H: 3.90.

Synthesis of $Cp_2TaH[(PCy)_2]$ (4). This compound was prepared from Cp_2TaH_3 and cyclohexylphosphine as described for compound **3**, giving yellow-brown crystals in 50% yield. ^{1}H NMR (C_6D_6): 4.63 (d, $|J_{P-H}| = 1$ Hz, 5H), 4.50 (s, 5H), 2.59 (m, 1H), 2.48 (m, 1H), 2.29 (m, 1H), 1.93−1.26 (m, 17H), 0.57−0.43 (m, 2H), −1.76 (d, $|J_{P-H}| = 41$ Hz, 1H). ^{13}C{^{1}H} NMR (C_6D_6): 92.1 (d, $|J_{P-C}| = 8$ Hz), 90.(d, $|J_{P-C}|$ 5Hz), 40.3−40.1 (m), 39.1 (dd, $|J_{P-C}| = 40$, 18 Hz), 34.8 (dd, $|J_{P-C}| = 26$, 6 Hz), 33.2 (dd, $|J_{P-C}| = 19$ Hz, 4 Hz), 28.2−27.5 (m); ^{31}P NMR (C_7H_8): −123.1 (dd, $|J_{P-P}| = 338$ Hz, $|J_{P-H}| = 30$ Hz), −143.3 (d, $|J_{P-P}| = 338$ Hz). Anal. Calcd for $C_{22}H_{33}P_2Ta$: C: 48.90; H: 6.15. Found: C: 48.60; H: 6.00.

Synthesis of $Cp_2TaH[(PH)_2]$ (5). A solution of Cp_2TaH_3 (400 mg, 1.27 mmol) and white phosphorus (120 mg, 0.968 mmol P_4) in toluene (10 mL) was heated overnight at 85 °C in a sealed flask. The solution was filtered through activated alumina to remove excess phosphorus and then evaporated to give an off-white powder (342 mg, 71% yield). Recrystallization from toluene at −35 °C gave small colorless crystals suitable for crystallography. ^{1}H NMR (C_7D_8, 233K, 500 MHz): δ 4.34 (d, $|J_{P-H}| = 1$ Hz, 5H), 4.24 (s, 5H), −0.23 (ddd, $|J_{P-H}| = 150$, 27 Hz, $|J_{H-H}| = 19$ Hz, 1H), −1.14 (ddd, $|J_{P-H}| = 146$, 21 Hz, $|J_{H-H}| = 19$ Hz, 1H), −2.36 (d, $|J_{P-H}| = 35$ Hz, 1H); ^{13}C{^{1}H} NMR (C_7D_8, 193K, 75 MHz): δ 91.03, 89.86; ^{31}P NMR (C_7H_8, 233K, 202 MHz) δ −268.03 (ddd, $|J_{P-P}| = 240$ Hz, $|J_{P-H}| = 150$, 21 Hz), −271.68 (dddd, $|J_{P-P}| = 240$ Hz, $|J_{P-H}| = 146$, 35, 27 Hz). Anal. Calcd for $C_{10}H_{13}P_2Ta$: C: 31.94; H: 3.48; Found: C: 31.75; H: 3.40.

EHMO and MMX Calculations. Extended Huckel molecular orbital (EHMO) and molecular mechanics (MMX) calculations were performed on a PowerMac 7100 workstation employing the CaChe software package.[14] Models were constructed on the basis of idealized geometries derived from related crystallographic data.

X-ray Data Collection and Reduction. X-ray quality crystals of **1**−**5** were obtained directly from the preparations described above. The crystals were manipulated and mounted in capillaries in a glove box, thus maintaining a dry, O_2-free environment for each crystal. Diffraction experiments for **1** and **2** were performed on a Rigaku AFC6 diffractometer equipped with graphite-monochromatized Mo Kα radiation, while X-ray data for **3**−**5** were obtained employing a Siemens SMART System CCD diffractometer collecting a hemisphere of data in 1329 frames with 10 s exposure times. In the former cases, the initial orientation matrix was obtained from 20 machine-centered reflections selected by an automated peak search routine. These data were used to determine the crystal systems. Automated Laue system check routines around each axis were consistent with the crystal system. Ultimately, 25 reflections ($20° < 2\theta < 25°$) were used to obtain the final lattice parameters and the orientation matrices. Crystal data are summarized in Table 1. The observed extinctions were consistent with the space groups in each case. The data sets were collected in three shells ($4.5° < 2\theta < 45-50.0°$), and three standard reflections were recorded every 197 reflections. Fixed scan rates were employed. Up to four repetitive scans of each reflection at the respective scan rates were averaged to insure meaningful statistics. The number of scans of each reflection was determined by the intensity. The intensities of the standards showed no statistically significant change over the duration of the data collections. The data were processed using the TEXSAN crystal solution package operating on a SGI Challenge mainframe computer with remote X-terminals. The reflections with $F_o^2 > 3\sigma F_o^2$ were used in the refinements.

(11) Allman, T.; Bain, A. D.; Garbow, J. R. *J. Magn. Reson.* **1996**, *123A*, 26.

(12) (a) Antinolo, A.; Chaudret, B.; Commenges, G.; Fajardo, M.; Jalon, F.; Morris, R. H.; Otero, A.; Schweltzer, C. T. *J. Chem. Soc., Chem. Commun.* **1988**, 1210. (b) Green, M. L. H.; Moreau, J. J. E. *J. Organomet. Chem.* **1978**, *161*, C25.

(13) Schrock, R. R.; Sharp, P. R. *J. Am. Chem. Soc.* **1978**, *100*, 2389.

(14) CaChe Worksystem Software is an integrated modeling, molecular mechanics, and molecular orbital computational software package and is a product of CaChe Scientific Inc.

Table 1. Crystallographic Parameters[a]

	1	2	3	4	5
formula	$C_{22}H_{21}P_2Nb$	$C_{28}H_{37}P_2Si_2Nb$	$C_{22}H_{21}P_2Ta$	$C_{22}H_{33}P_2Ta$	$C_{10}H_{13}P_2Ta$
fw	440.26	584.63	528.30	540.37	376.11
a, Å	6.462(3)	17.098(6)	6.4990(8)	12.2495(1)	13.225(5)
b, Å	15.434(3)	15.134(7)	15.382(2)	9.9566(1)	7.876(3)
c, Å	19.996(2)	11.759(6)	20.006(3)	17.6905(3)	22.139(8)
β, deg				90.385(1)	102.931(3)
V, Å^3	1994(1)	3042(3)	1999.9(4)	2157.54(5)	2247(1)
space group	*Pbcn*	$Pna2_1$	*Pbcn*	*I*2/*a*	$P2_1/c$
D(calc), g cm^{-3}	1.47	1.28	1.75	1.664	2.22
Z	4	4	4	4	8
μ, cm^{-1}	7.37	5.93	56.49	52.46	100.03
scan speed, deg/min	8.0	8.0	na	na	na
data collected	2064	3044	1430	5254	5413
2θ/index ranges	4.5−50	4.5−50	4.5−50	4.5−56.6	4.5−50
data $F_o^2 > 3\sigma(F_o^2)$	720	452	624	2232	4041
no. of variables	117	87	59	117	235
transmission factors	0.87−1.00	0.38−1.00	0.65−1.00	0.56−1.00	0.69−1.00
R (%)	4.8	7.8	7.9	3.45	6.3
R_w(%)	3.0	7.3	7.4	4.18	7.6
goodness of fit	1.54	2.52	2.34	1.38	2.22

[a] Data collected at 24 °C with Mo Kα radiation (λ = 0.710 69 Å), $R = \sum||F_o| - |F_c||/\sum|F_o|$, $R_w = [\sum(|F_o| - |F_c|)^2/\sum|F_o|^2]^{0.5}$.

Structure Solution and Refinement. Non-hydrogen atomic scattering factors were taken from the literature tabulations.[15,16] The heavy atom positions were determined using direct methods employing either the SHELX-86 or Mithril direct methods routines. The remaining non-hydrogen atoms were located from successive difference Fourier map calculations. The refinements were carried out by using full-matrix least squares techniques on F, minimizing the function $\omega(|F_o| - |F_c|)^2$ where the weight ω is defined as $4F_o^2/2\sigma(F_o^2)$ and F_o and F_c are the observed and calculated structure factor amplitudes. In the final cycles of each refinement, the number of non-hydrogen atoms assigned anisotropic temperature factors was determined so as to maintain a reasonable data: variable ratio. The remaining atoms were assigned isotropic temperature factors. In some instances the geometries of the cyclopentadienyl and phenyl rings were also constrained to maintain a statistically meaningful data:variable ratio. Empirical absorption corrections were applied to the data sets based either on ψ-scan data or a DIFABS calculation and employing the software resident in the TEXSAN package. Hydrogen atom positions were calculated and allowed to ride on the carbon to which they are bonded assuming a C−H bond length of 0.95 Å. Hydrogen atom temperature factors were fixed at 1.10 times the isotropic temperature factor of the carbon atom to which they are bonded. The hydrogen atom contributions were calculated, but not refined. In the case of **4**, the cyclopentadienyl ring was refined as a constrained, rigid pentagon group with individual atomic thermal parameters. Where appropriate the correct enantiomorph of the models was confirmed by inversion and refinement of the model. The final values of R, R_w, and the goodness of fit in the final cycles of the refinements are given in Table 1. The locations of the largest peaks in the final difference Fourier map calculation as well as the magnitude of the residual electron densities in each case were of no chemical significance. Positional parameters, hydrogen atom parameters, thermal parameters, and bond distances and angles have been deposited as Supporting Information.

Results and Discussion

Synthesis and Reactivity. The reaction of Cp_2NbH_3 with excess phenylphosphine was performed in toluene. Monitoring the reaction at 25 °C showed no reaction over the course of 24 h. In contrast, brief heating of the mixture to 80 °C resulted in the observation of new resonances in the ^{31}P NMR in addition to that of free phosphine. Upon cooling to −35 °C, bright yellow crystals of **1** were obtained from the reaction mixture. The $^{31}P\{^1H\}$ NMR of **1** showed two doublets at −107.45 and −124.80 ppm with $|J_{P-P}| = 353$ Hz consistent with two distinct yet coupled phosphorus environments. The ^{1}H NMR spectrum of **1** contains resonances at 4.48 and 4.32 attributable to two cyclopentadienyl rings. The resonance at −1.63 ppm which shows coupling to phosphorus of 51.0 and 3.5 Hz is attributed to a Nb hydride. Thus, based on these spectroscopic data, **1** is formulated as $Cp_2NbH[(PPh)_2]$. Subsequently the reaction was performed employing the appropriate stoichiometry, and **1** was obtained in 73% isolated yield. Two possible structural isomers of **1** are consistent with the spectroscopic data. These correspond to *cisoid* and *transoid* arrangements of the phenyl rings with respect to the NbP_2 ring. An X-ray crystallographic study of **1** (Figure 1) confirmed a *transoid* configuration of the phenyl rings.

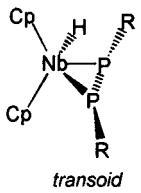

transoid

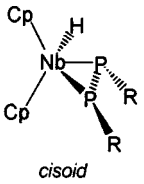

cisoid

The analogous reactions of phenylphosphine with Cp'_2NbH_3 or Cp_2TaH_3 afford the products, $Cp'_2NbH[(PPh)_2]$ (**2**) and $Cp_2TaH[(PPh)_2]$ (**3**), respectively. Similarly, the reaction of cyclohexylphosphine and Cp_2TaH_3 affords the diphosphanato complex $Cp_2TaH[(PCy)_2]$ (**4**). These species **2**−**4** were also characterized crystallographically (Figures 1−3). In all cases, *transoid* dispositions of the substituents on the diphosphanato moiety were confirmed.

Compound **3** was previously obtained by Moise *et al.*[9] from the reaction of diphenylphosphine and Cp_2TaH_3. In that case, an intermediate phosphide−dihydride complex $Cp_2TaH_2(PPh_2)$ was postulated. In the present

(15) (a) Cromer, D. T.; Mann, J. B. *Acta Crystallogr. Sect. A: Cryst. Phys., Theor. Gen. Crystallogr.* **1968**, *A24*, 324. (b) Cromer, D. T.; Mann, J. B. *Acta Crystallogr. Sect. A: Cryst. Phys., Theor. Gen. Crystallogr.* **1968**, *A24*, 390.

(16) Cromer, D. T.; Waber, J. T. *International Tables for X-ray Crystallography*; Knoch Press: Birmingham, England, 1974.

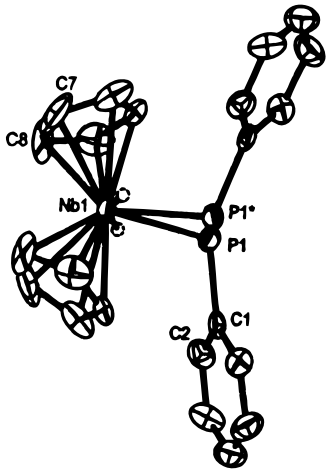

Figure 1. ORTEP drawing of **1**; 30% thermal ellipsoids are shown. Disordered hydride atom positions are shown. Nb(1)−P(1) 2.644(2) Å; P(1)−P(1) 2.136(5) Å; P(1)−Nb(1)−P(1) 47.6(1)°. The compound **3** is isostructural, Ta(1)−P(1) 2.634(7) Å; P(1)−P(1) 2.17(2) Å; P(1)−Ta(1)−P(1) 48.8(4)°.

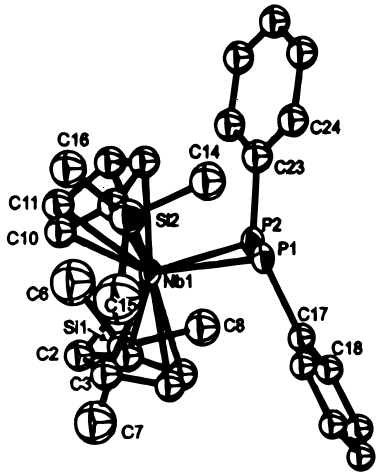

Figure 2. ORTEP drawing of **2**; 30% thermal ellipsoids are shown. Nb(1)−P(1) 2.66(1) Å; Nb(1)−P(2) Å; 2.60(2) P(1)−P(2) 2.16(3) Å; P(1)−Nb(1)−P(2) 48.4(7)°.

case, it is reasonable to suggest the analogous species $Cp_2MH_2(PHPh)$ is formed initially in the reaction sequence. What is unclear is how the reaction proceeds from there. Loss of H_2 could generate a phosphinidene intermediate which subsequently reacts with more phosphine to yield a diphosphide complex which is subsequently transformed to the diphosphanato product. (Scheme 1, route a). This mechanism would be in accord with that postulated for related Zr−P chemistry.[3] An alternative pathway could involve loss of H_2 from a diphosphide intermediate $Cp_2TaH(PHR)_2$ (Scheme 1, route b). However, this view is invalidated by the observation that the reactions of Cp_2TaMe_3 or Cp_2TaMe_2Br and PH_2Ph also afford **3** (R = H) as the major product, which further supports the proposal of a transient phosphinidene intermediate. Nonetheless, attempts to intervene in these reactions to confirm the intermediacy of a phosphinidene complex have been unsuccessful to date. Unequivocal clarification of the operative mechanism awaits further study.

An alternative synthetic route to the primary diphosphanato complex $Cp_2TaH[(PH)_2]$ (**5**) was discovered. Reaction of Cp_2TaH_3 with P_4 in hot toluene leads to an initially dark solution from which an off-white powder

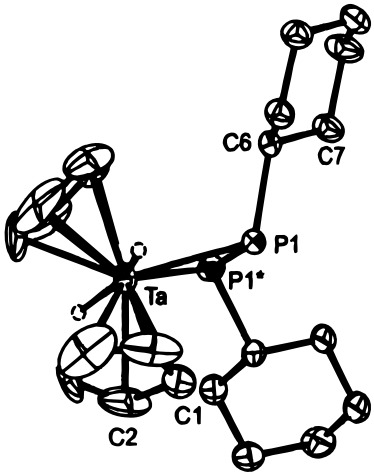

Figure 3. ORTEP drawing of **4**; 30% thermal ellipsoids are shown. Disordered hydride atom positions are shown. Ta(1)−P(1) 2.623(1) Å; P(1)−P(1) 2.131(3) Å; P(1)−Ta(1)−P(1) 47.94(6) °.

Scheme 1

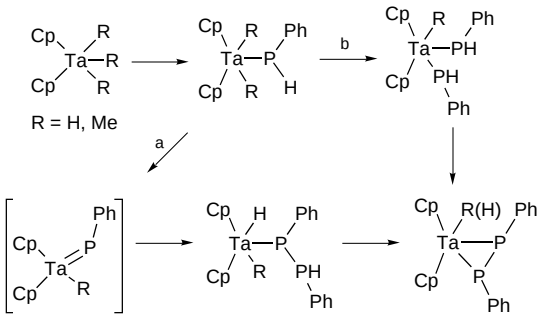

was isolated via filtration through alumina. The initial ^{31}P NMR spectral data obtained at 80 MHz and 25 °C for this isolated product **5** revealed a single resonance at −289.2 ppm, while the ^1H NMR data suggested the presence of two cyclopentadienyl ligand environments. These observations suggested fluxional behavior and prompted a variable temperature NMR study (*vide infra*). Confirmation of the formulation of **5** as $Cp_2TaH[(PH)_2]$ was achieved by X-ray crystallography (Figure 4). It is noteworthy that Green et al. prepared $Cp_2Mo[(PH)_2]$ via the same route employing Cp_2MoH_2 and P_4.[17]

Attempts to effect the catalytic activation of primary phosphines by the reaction of the above diphosphanato complexes **1**−**5** at up to 110 °C in toluene were unsuccessful. These complexes are robust under these conditions, unlike the analogous Zr anions. Compound **3** did react stoichiometrically with $PhPCl_2$ at 80 °C to afford $(PPh)_5$. The presumed reaction pathway involves an initial metallacyclic transfer reaction giving $(PPh)_3$ which subsequently undergoes thermal redistribution.

Structural Studies. Structural data for **1**−**5** reveal similar geometry features. The coordination spheres of these compounds consist of two π-bonded cyclopentadienyl ligands with a $(PR)_2$ fragment bonded to the metal center forming a tight MP_2 three-membered ring with P−M−P angles in the range from 47.6−48.4°. Single hydride ligands complete the coordination spheres. In

(17) (a) Green, J. C.; Green, M. L. H.; Morris, G. E.; *J. Chem. Soc., Chem. Commun.* **1974**, 212. (b) Cannillo, E.; Coda, A.; Prout, K.; Daran, J. C. *Acta Crystallogr. B.* **1977**, *33*, 2608.

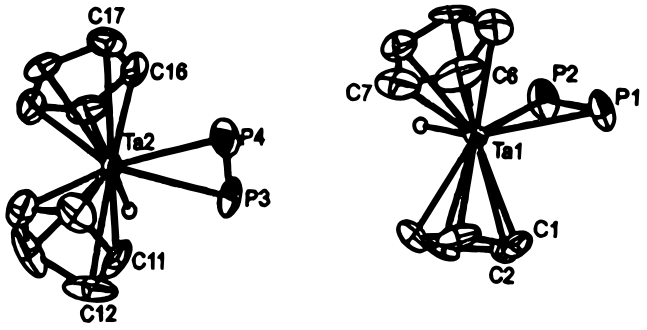

Figure 4. ORTEP drawing of the two molecules of **5** in the asymmetric unit; 30% thermal ellipsoids are shown Ta(1)−P(1) 2.632(5) Å; Ta(1)−P(2) 2.602(5) Å; Ta(2)−P(3) 2.586(3) Å; Ta(2)−P(4) 2.627(4) Å; P(1)−P(2) 2.138(6) Å; P(3)−P(4) 2.136(6) Å; P(1)−Ta(1)−P(2) 48.2(1)^0; P(3)−Ta(2)−P(4) 48.4(1)°.

the case of compounds **1** and **3**−**5** the hydride was located and in the case of **4** refined. For **1**, **3**, and **4**, the hydride position was disordered, generating a pseudo-two-fold axis of symmetry. The substituents on P adopt a *transoid* disposition in **1**−**4**. In the case of **5** the hydrogen atoms on P could not be located, and thus their disposition in the solid state remains unknown. The chemically inequivalent M−P distances in each of **1**, **3**, and **4** are indistinguishable as a result of disordered packing in the solid state. In the case of **2** the Nb−P distances differ slightly at 2.66(1) and 2.60(2) Å. This difference may result from a steric interaction as a result of the proximity of the trimethylsilyl substituent (Si(2)) to P(1). In compound **5**, the Ta−P distances which average 2.612(5) Å are shorter than those seen in **3** consistent with the increased basicity of the $(PH)_2$ versus the $(PPh)_2$ fragment. In all compounds, P−P distances are typical ranging from 2.138(5)−2.17(2) Å.

The structural data are consistent with a minimal stereochemical role of the hydride ligand. EHMO calculations support the notion that the metal−hydride bonding arises from interaction of the H 1s orbital with the $1a_1$ orbital of the Cp_2M fragment (as shown). As this fragment orbital is essentially parallel to the P−P vector, the hydride ligand is expected to exhibit little

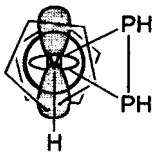

effect on the complex geometry. This view is supported by the observation of disordered packing of **1**, **3**, and **4** despite the molecular dissymmetry.

Variable Temperature NMR Studies. The variable-temperature ^1H and ^{31}P NMR spectra of **5** exhibit a variety of fascinating changes, as shown in Figures 5 and 6. In the ^1H regime at 233 K, the high-field region exhibits two multiplets, at −0.15 and −1.05 ppm, assigned to the $(PH)_2$ fragment, and a somewhat broadened doublet ($|^2J_{P-H}| \approx 35$ Hz) at −2.24 ppm attributable to the metal hydride. The multiplet at −0.15 consists of a doublet ($|^1J_{P-H}| = 150$ Hz) of doublets ($|^2J_{P-H}| = 27$ Hz) of doublets ($|^3J_{H-H}| = 19$ Hz); similarly, the other multiplet at −1.05 ppm is a doublet ($|^1J_{P-H}| = 146$ Hz) of doublets ($|^2J_{P-H}| = 21$ Hz) of doublets ($|^3J_{H-H}| = 19$ Hz). Lowering the temperature to 193 K

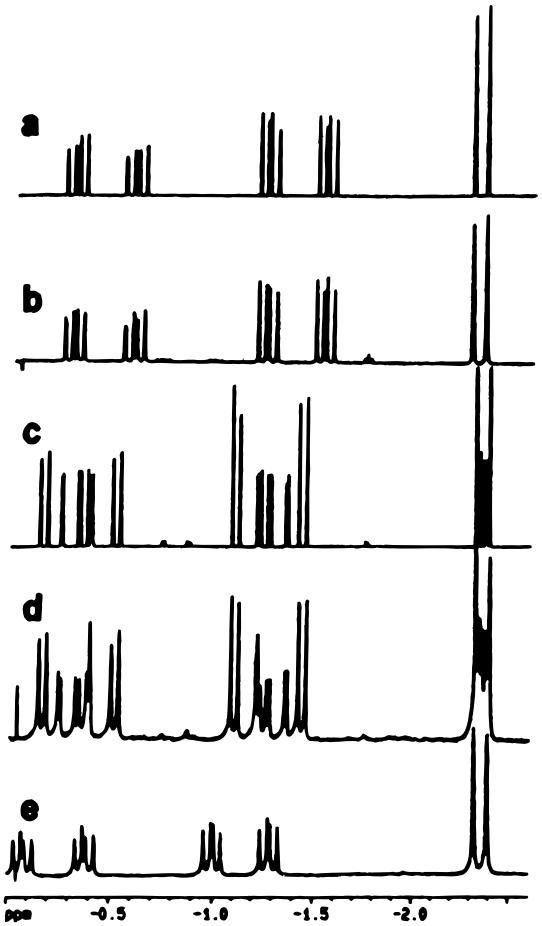

Figure 5. Variable temperature experimental and simulated ^1H NMR spectra of **5**: (a) simulation of spectrum at 340 K, (b) experimental spectrum at 340 K, (c) simulation of spectrum at 273 K, (d) experimental spectrum at 273 K, (e) experimental spectrum at 233 K.

reveals no substantive changes except for additional broadening of all peaks. In contrast, as the temperature is raised to 375 K, the two multiplet resonances centered at −0.15 and −1.05 ppm not only move gradually (to −0.44 and −1.48 ppm, respectively) but also become much more complicated (between 273 K and 303 K) before eventually recovering their original eight-line patterns; moreover, above 300 K, the multiplet at −0.4 ppm shows a 2 Hz coupling to the tantalum hydride.

Even more dramatic is the behavior exhibited by the ^{31}P spectra over the range 193 K to 375 K. At the lowest temperature, we see a doublet ($|^1J_{P-P}| = 240$ Hz) of doublets ($|^1J_{P-H}| = 150$ Hz) of doublets ($|^2 J_{P-H}| = 21$ Hz) at −267.4 ppm, and a doublet ($|^1J_{P-P}| = 240$ Hz) of doublets ($|^1J_{P-H}| = 146$ Hz) of pseudo-triplets ($|^2J_{P-H}| = 27$ Hz; $|^2J_{P-(Ta)H}| \approx 35$ Hz) at −274.5 ppm. As the temperature is raised there is a rather small effect on the −267.4 ppm peak which moves upfield by approximately 1 ppm; however, the 12-line pattern, originally centered at −274.5 ppm marches steadily downfield to −264.8 ppm. This is most clearly seen in the proton decoupling 31P spectra shown in Figure 6. Over the range 273−303 K, there is severe overlap between the two ^{31}P resonances, and this is the cause of the very marked second-order effects which are apparent in the proton NMR spectra over this same temperature range.

At low (233 K) or high (375 K) temperatures the ^1H and ^{31}P spectra of **5** are readily rationalizable as

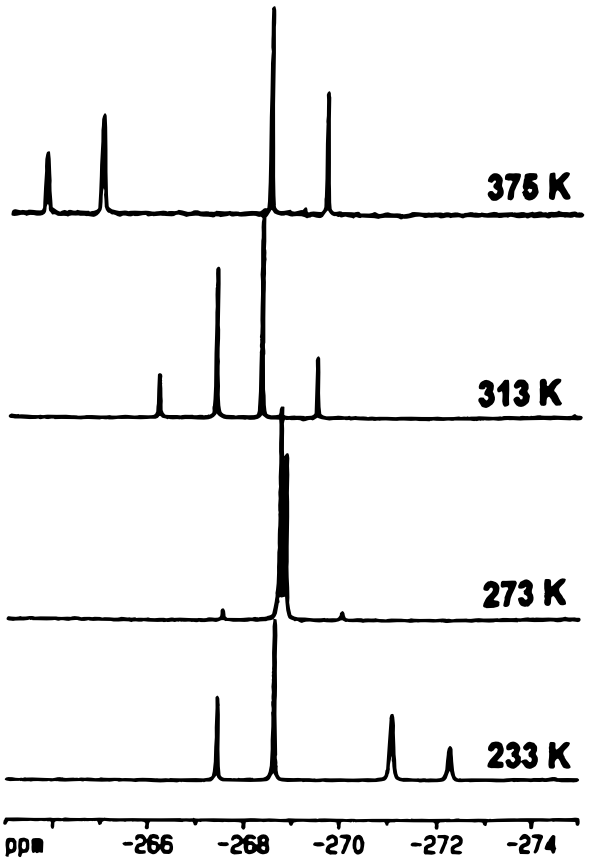

Figure 6. Variable temperature $^{31}P\{^1H\}$ NMR spectra of **5**.

straightforward first-order multiplets. At 303 K, however, the temperature-dependent shift of the "central" ^{31}P nucleus causes it to overlap with the resonance assigned to the "outer" phosphorus environment. This results not merely in a complex ^{31}P NMR spectrum but also induces severe second-order effects in the ^1H resonances of the Ta−H and HP−PH fragments.

To verify that the plethora of extra peaks in the room temperature ^1H NMR spectra of **5** is indeed the result of the change in ^{31}P chemical shift differences, the spectra were simulated with use of the program SIMPLTN.[11] In this procedure, the chemical shift difference between the ^{31}P resonances was systematically changed to match the experimental ^{31}P NMR data, and the ^1H and ^{31}P spectra were simulated for each case.

Figure 5 shows experimental and simulated ^1H spectra at 340 K (when the ^{31}P resonances are widely separated) that contrast with the experimental and simulated ^1H spectra at 273 K (when the ^{31}P peaks are severely overlapped). Figure 7 shows the experimental and simulated ^{31}P spectra at 273 K.

These temperature-dependent effects are also dramatically apparent in the 2D spectra at different temperatures. In the unsymmetrized experimental $^1H-^1H$ COSY spectrum of **5** at 353 K only the expected off-diagonal peaks are visible. This should be contrasted with Figure 8, which depicts the experimental and simulated $^1H-^1H$ COSY spectra of **5** at 303 K when ^{31}P-mediated interactions between all the proton environments are now evident. The mechanism by which these effects are propagated will be the subject of a future submission.

The attribution of the ^{31}P resonances to *proximal* (P_a) and *distal* (P_b) environments, relative to the tantalum

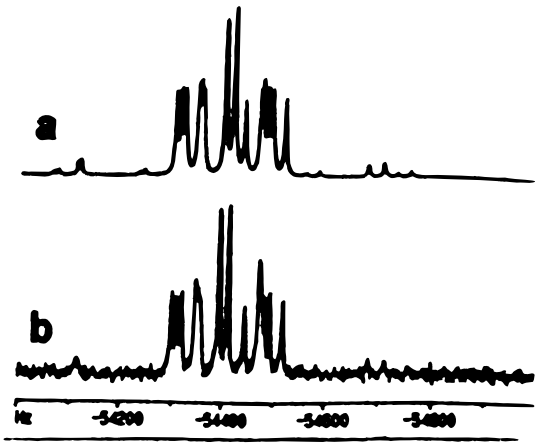

Figure 7. (a) Simulated and (b) experimental ^{31}P NMR spectra of **5** at 273 K.

hydride with which they are coplanar, is based on the observation of coupling of only one of the phosphorus nuclei to the Ta−H. Although one might expect sizeable $|^2J_{H-M-P}|$ interactions to be favored when the H−M−P angle is relatively large, and thus conclude that the *distal* phosphorus couples to the metal hydride, 2D NOESY spectra at 353 K show a clear NOE from the Ta−H to the PH at −0.43 ppm and a much smaller enhancement to the PH resonance at −1.38 ppm. Selective decoupling experiments at 353 K show clearly that the ^1H resonance at −0.43 ppm is attributable to the P−H moiety that gives rise to the ^{31}P resonance at −266 ppm. Likewise, the ^1H resonance at −1.38 ppm is assignable to the P−H unit with a ^{31}P chemical shift of −269ppm. This supports the assignment of the PH resonance at −0.43 ppm to the "central" PH group, and thus it is the central P environment that undergoes the large temperature dependent shift (P_aH_a).

The X-ray crystal structure of the analogous complexes **1**−**4** revealed that, at least in the solid state, the two P substituents adopt a *transoid* orientation with respect to the MP_2 ring. However, the X-ray data for **5** do not unequivocally define the relative positions of the hydrogen substituents. Nevertheless, the structure adopted by **5** at 193 K was readily ascertained by means of nuclear Overhauser difference measurements in the ^1H NMR spectra. The two cyclopentadienyl rings give rise to proton resonances at 4.34 and 4.24 ppm; irradiation of the former Cp rings shows clear NOE enhancement of the PH peak at −0.15 ppm (H_a), while the Cp ring at 4.24 ppm connects similarly to the PH absorption at −1.05 ppm (H_b). Since these phosphorus-bonded hydrogens are each proximate to only one cyclopentadienyl ring, one can conclude that they are *transoid* to each other.

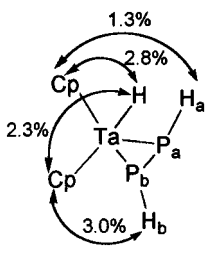

On first consideration, one might attempt to rationalize these variable-temperature NMR data to be based on the proposition of some fluxional process. For

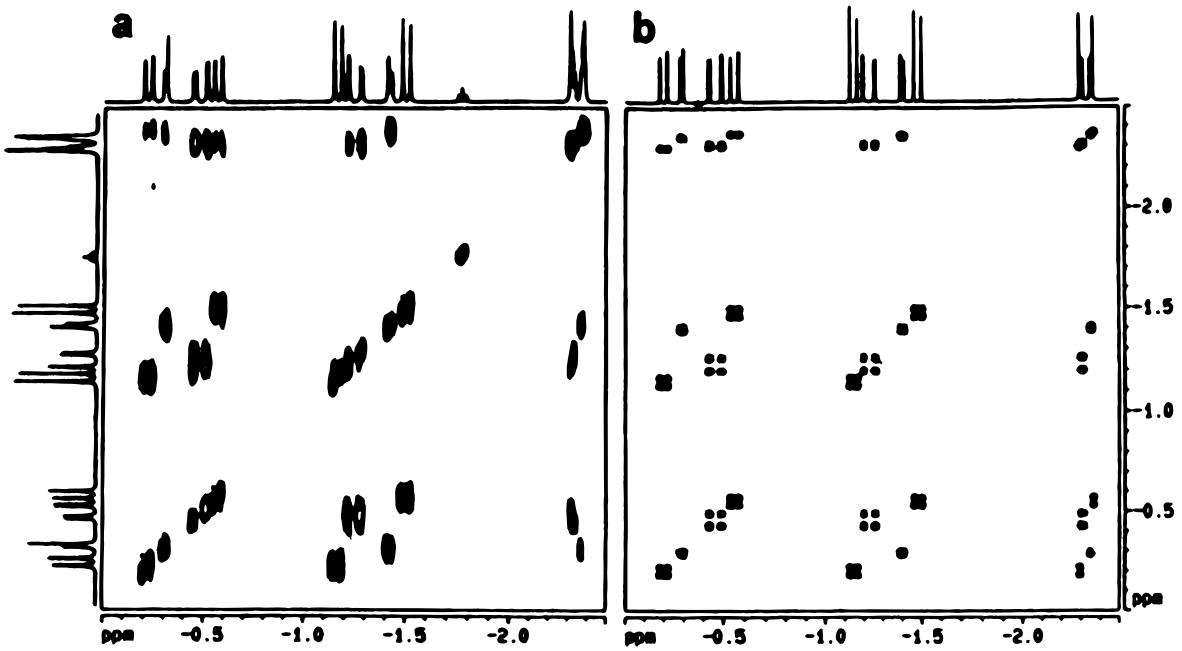

Figure 8. (a) Experimental and (b) simulated $^{1}H-^{1}H$ COSY spectra of **5** at 303 K.

example, one might consider temperature dependent equilibria between *cisoid* and *transoid* isomers of **5** which are interconverted via P inversion. We note, however, that inversion of both PH moieties would have led to equilibrium of the Cp environments, but experimentally this phenomenon is never realized. Energy minimization calculations based on molecular mechanics were performed on models for both the *cisoid* and *transoid* isomers of **5**. The total energy difference for the optimized structures was 1−2 kcal/mol, consistent with the proposition of an equilibrium process. However, examination of the variable temperature ^{31}P NMR spectra for **1** and **3** revealed a similar temperature dependence of the chemical shifts. In the case of **3**, although the two signals never overlap, one of the resonances gradually migrates from −152 to −139 ppm while the other is relatively constant between −164 and −160 ppm. The similar magnitudes in chemical shift changes for the analogous compounds, **1**, **3**, and **5**, suggest a common explanation. It would seem unlikely that a fluxional process involving P inversion would occur to the same extent for both the H- and phenyl-substituted analogs. Thus we are left to conclude that these compounds exhibit an unusual and perplexing chemical shift temperature dependence.

Acknowledgment. Financial support from the NSERC of Canada to D.W.S., A.D.B., and M.J.M. is gratefully acknowledged. Professor Antonio Otero of Universidad de Castilla−La Mancha is thanked for the gift of 5 g of Cp'_2NbCl_2. Financial support for M.B. from NSF (Grant No. CHE9314732) to T. Cundari, Memphis University, is gratefully acknowledged. The technical assistance of Dr. Howard Hunter (Bruker) and Dr. D. W. Hughes (McMaster University) is also gratefully acknowledged.

Supporting Information Available: Tables of crystallographic parameters, atom coordinates, and thermal parameters (18 pages). Ordering information is given on any current masthead page.

OM970189W